APL Materials

Atomic-resolution analytical scanning transmission electron microscopy of topological insulators with a layered tetradymite structure

Cite as: APL Mater. 8, 070902 (2020); https://doi.org/10.1063/5.0014113
Submitted: 18 May 2020 . Accepted: 29 June 2020 . Published Online: 10 July 2020

Danielle Reifsnyder Hickey, and K. Andre Mkhoyan

Atomic-resolution analytical scanning transmission electron microscopy of topological insulators with a layered tetradymite structure

Cite as: APL Mater. 8, 070902 (2020); doi: 10.1063/5.0014113
Submitted: 18 May 2020 • Accepted: 29 June 2020 •
Published Online: 10 July 2020

Danielle Reifsnyder Hickey[1,a] and K. Andre Mkhoyan[2,a]

AFFILIATIONS

[1] Department of Materials Science and Engineering, The Pennsylvania State University, University Park, Pennsylvania 16802, USA
[2] Department of Chemical Engineering and Materials Science, University of Minnesota, Minneapolis, Minnesota 55455, USA

[a] Authors to whom correspondence should be addressed: drh283@psu.edu and mkhoyan@umn.edu

ABSTRACT

The recent discovery of topological insulators has uncovered exciting new quantum materials with potential applications in the emergent fields of topological spintronics and topological quantum computation. At the heart of uncovering the new physical properties of these materials is the characterization of their atomic structures, composition, defects, and interfaces. The technique of atomic-resolution analytical scanning transmission electron microscopy has already provided many insights and holds great promise for future discoveries. This perspective discusses advances that have been achieved in the atomic-scale characterization of topological insulators with a layered tetradymite structure, and it proposes future directions to link atomic-scale features to exciting new physical phenomena.

INTRODUCTION

Topological insulators (TIs) have emerged as fascinating quantum materials[1,2] that have led to renewed interest in the tetradymite family of Bi,Sb-chalcogenides [e.g., Bi_2Se_3, Bi_2Te_3, Sb_2Te_3, $(Bi,Sb)_2Te_3$, etc.].[3,4] For example, bismuth chalcogenides offer efficient spin-to-charge conversion because they have large spin–orbit coupling and spin–momentum locking of surface states,[2,5] generate a spin–transfer torque,[6,7] undergo current-induced spin polarization,[8] and exhibit ferromagnetic resonance-driven room-temperature spin pumping.[9] This workhorse system has also garnered interest due to its layered crystal structure: similar to graphene, transition metal dichalcogenides, and other two-dimensional (2D) materials, tetradymites consist of layers that are covalently bonded in the *a*–*b* plane and separated by van der Waals bonding in the *c*-direction. However, unlike for other 2D materials, each tetradymite layer is a five-atom-thick quintuple layer (QL). The identification and characterization of the dominant defects in Bi,Sb-chalcogenides are critical for emerging technologies based on their exotic properties. Therefore, analytical scanning transmission electron microscopy (STEM) is an ideal technique for elucidating these defects. Unlike many characterization techniques that provide either bulk (e.g., x-ray diffraction) or hundreds-of-nanometer- to micrometer-scale information (e.g., x-ray photoelectron spectroscopy, Raman spectroscopy, and atomic force microscopy), STEM makes it possible to perform local analysis on the Angstrom scale.

Atomic-resolution imaging via annular dark-field STEM (ADF-STEM) and accompanying elemental mapping using energy-dispersive x-ray (EDX) spectroscopy and electron energy-loss spectroscopy (EELS) have been instrumental in identifying and characterizing a variety of defects in TIs. These defects span across dimensionalities, from point (0D) to line (1D), planar (2D), and volume (3D) defects. In STEM, when aberrations of the lenses are corrected, a focused electron beam (<1 Å) interacts with a thin (<100 nm) sample in transmission mode to create mostly elastically scattered electrons that are used to directly image atomic positions.[10–12] The scattered electrons are collected by an annular detector with intensities proportional to Z^n, where Z is the atomic number of the element imaged, and the exponent n is in the range of

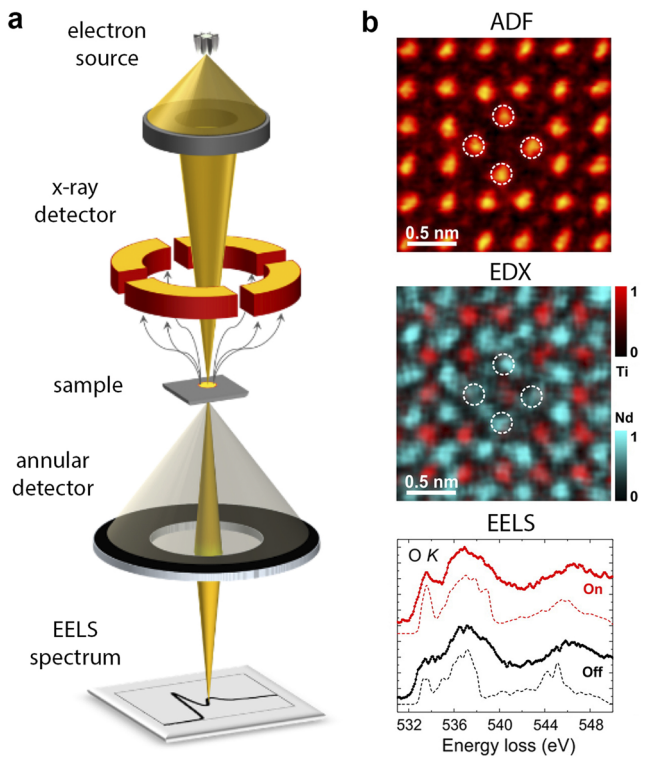

FIG. 1. (a) A simple ray diagram describing the geometry of the ADF detector and EDX and EELS systems in STEM.[23] (b) A magnified ADF image of a line defect in $NdTiO_3$, along with an EDX spectrum-image composed of the Nd and Ti *L* signals. The positions of Nd columns in the defect core are indicated by dashed circles. EELS data for the O *K*-edge, measured on and off a defect site are also shown.[24]

1.2–2.0.[13–16] The electron probe is then rastered across the sample to collect these images, simultaneously producing x rays characteristic of core electron states[17] and low-angle inelastically scattered electrons, which are used to create EDX and EELS signals, respectively (Fig. 1).[18–22] As a result, analytical STEM is an unparalleled source of detail about the atomic structure and composition of defects in materials.

PROGRESS TO DATE

Analytical STEM is an excellent technique for the study of crystalline defects and interfaces, where local information about a material is critical. Not surprisingly, it has yielded numerous insights into structural distortions in a variety of tetradymite TIs. Although STEM is capable of detecting and characterizing defects of all dimensions, the majority of the existing body of work on tetradymite TIs is focused on 2D defects and interfaces. Due to similar energies, the atoms in rhombohedral Bi,Sb-chalcogenide TIs (space group $R\bar{3}m$) can stack in either ABC or ACB geometries. This commonly gives rise to twinning, which is equivalent to a 60° rotation of the tetradymite crystal structure. When the stacking order changes from ABC to ACB within a single grain as it grows along the crystallographic *c*-axis, a basal (lamellar) twin forms. Such twins frequently have been observed in Bi_2Se_3[25–28] and Bi_2Te_3[29–32] [Fig. 2(a)]. Density functional theory (DFT) calculations for Bi_2Te_3 predict that this twin is favored to occur within the van der Waals gap between the QLs, rather than within the covalently bonded QL.[29] Moreover, a location-sensitive reduction of the bandgap is predicted for Bi_2Se_3 thin films with basal twins.[28] Atomic-resolution ADF-STEM images have enabled the identification of these basal twin locations in thin films[28] and nanowires,[33] as well as the quantification of the van der Waals gap expansion due to basal twinning.[29]

In addition, ADF-STEM imaging has enabled the discovery of other, less common stacking-related defects within these TI films. For instance, the substrate steps have been shown to create threading defects,[30] and the associated domain boundaries have been correlated with electrostatic fields that locally charge Dirac states.[33] Stacking faults can also lead to the insertion of regular arrays of extra atoms between M_2X_3 QLs[34,35] [Fig. 2(b)]. This can create disorder[34] or else produce different stoichiometries, such as Bi_1Te_1[35] [Fig. 2(c)]. Understanding such deviations in the atomic structure is particularly important because of how the structure alters the physical properties: Bi_1Te_1 has been identified to be a dual topological insulator, in which a weak topological insulator phase and a topological crystalline insulator phase coexist.[35]

In tetradymite TI films, when two adjacent grains possess dissimilar stacking orders, a rotational twin results [Fig. 2(d)]. In the case of Bi_2Te_3, these rotational twins have been reported to act as "structural doping" because the changes in the interatomic distance at the grain boundary create occupied states within the bandgap.[36] This free-electron creation increases the density of states near the conduction band minimum and reduces the electron mobility, which has important implications for devices. Such rotational twins have been observed and characterized using STEM in both Bi_2Se_3[25,26] and Bi_2Te_3[30,32,36] films.

Atomic-level insights into the interfaces in tetradymite materials are especially important because of the role of metallic surface states in TIs.[8,43,44] Of particular interest is the interface between tetradymite thin films and their growth substrates because it provides clues about how to engineer defect-free films. Because tetradymite films grow by van der Waals epitaxy, they do not require strict lattice matching with the substrate. As such, they have been grown on a variety of 3D substrates, such as (111)-oriented Si,[25,30,32,45,46] InP,[25,26,43,47,48] GaAs,[49] and $SrTiO_3$,[8] and (001)-oriented GaAs,[38] AlN,[50] and Al_2O_3.[27,51,52] When studied with STEM, some interfaces have been shown to be atomically sharp,[43,44,53,54] but in many cases, the interfacial region has been observed to be poorly crystalline [Fig. 2(e)] or contain nanoscale grains,[25,28,47,55] or to have a chalcogen-rich layer[30,37,38,49,52,56] [Figs. 2(f) and 2(g)]. In contrast, tetradymites grown on 2D materials, such as graphene,[57,58] hexagonal boron nitride,[39] and others,[59,60] possess mostly atomically sharp interfaces. In the special case of an Sb_2Te_3/Bi_2Te_3 interface, elemental intermixing has even been observed over a distance of several QLs.[61,62]

STEM imaging and spectroscopy provide otherwise unattainable local information about 3D structures and their compositional variations within tetradymites. For example, it was discovered that the $Fe_xCu_{1-x}Se$ tetragonal inclusions are single-crystalline and epitaxially oriented in the hexagonal structure of Bi_2Te_3, despite large (~20%) lattice mismatch.[63] STEM analysis has also shown that dopants and matrix elements sometimes segregate at grain

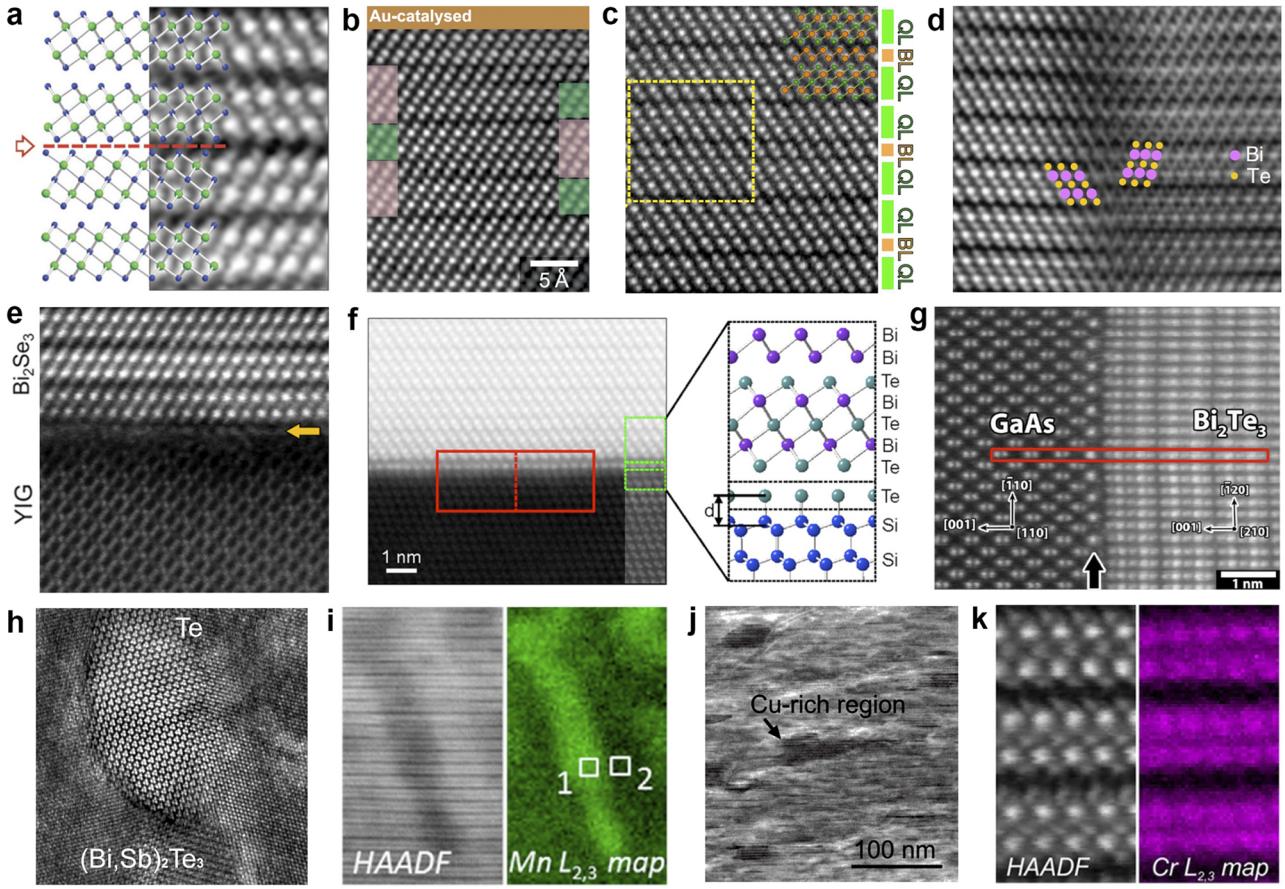

FIG. 2. (a) ADF-STEM image of a Bi_2Se_3 thin film containing a basal twin, with a model overlaid to show the details of the atomic arrangement of the twin.[28] (b) ADF-STEM image of a Bi_2Te_3 nanowire catalyzed by Au particles: the irregular stacking of QLs and septuple layers are visible.[34] (c) ADF-STEM image of Bi_1Te_1, which is a superlattice of QLs and Bi bilayers.[35] (d) ADF-STEM image of a 60° rotational twin boundary in Bi_2Te_3.[36] (e) Cross-sectional ADF-STEM image of an MBE-grown Bi_2Se_3 film showing a disordered heavy-atom layer at the Bi_2Se_3/YIG interface (indicated by a yellow arrow).[28] (f) ADF-STEM image and the atomic model of a Te layer present at a Bi_1Te_1/Si(111) interface.[37] (g) ADF-STEM image of a Bi_2Te_3/GaAs interface containing interfacial Ga_2Te_3.[38] (h) ADF-STEM image of a Te pocket at a grain boundary in a $(Bi,Sb)_2Te_3$ thin film.[39] (i) ADF-STEM image of Mn-doped Bi_2Te_3 (left) and Mn $L_{2,3}$ EELS map (right), suggesting that Mn can substitute at the Te site.[40] (j) ADF-STEM image of Cu-rich precipitates surrounded by a lower-Cu-content matrix in heavily Cu-doped Bi_2Se_3.[41] (k) ADF-STEM image of Cr-doped Bi_2Se_3 (left) and the atomically resolved Cr $L_{2,3}$ EELS map (right), showing that Cr substitutes at Bi sites.[42]

boundaries[39,42] [Fig. 2(h)] and that inclusions that form a secondary phase can be surrounded by interfaces with deteriorated crystallinity[40] [Fig. 2(i)]. Cu-rich precipitates in a lower-Cu-content doped Cu:Bi_2Se_3 matrix present yet another unusual case, where excess Cu is accommodated by intercalation into the van der Waals gap, leading to disorder, stacking faults, strain, and bending of the QLs[41] [Fig. 2(j)]. Dopant atoms have been identified in tetradymites to occupy multiple atomic positions in the host crystal, as well as to create disorder. Direct imaging with ADF-STEM and compositional analysis with EELS have revealed, for instance, that Cr is a substitutional dopant on the cation Bi,Sb sites in $(Bi,Sb)_2Te_3$, retaining the overall film stoichiometry without Cr segregation inside the film[64] [Fig. 2(k)], although Cr segregation has been observed for Bi_2Se_3 films.[42] In contrast, Mn dopants in Bi_2Te_3 have been observed to substitute for either the Bi cation or, for high Mn doping levels, for the Te anion, as well as to intercalate into the van der Waals gap and at the substrate interface.[40] Other dopants, such as K and Cu, have been reported to intercalate into the van der Waals gap between QLs, creating dislocations and stacking faults.[41,65]

The exact composition and the defects in the structure can have a significant impact on the physical properties of these TI materials. For example, in the case of Cu:Bi_2Se_3, various Cu-doped structures identified directly by atomic-resolution imaging have been shown to have different dielectric properties.[41] In the case of Bi_2Se_3 thin films containing basal twins, it is predicted that the presence of twins will result in opening the electronic bandgap.[28,29] Additionally, strain arising from dislocations and low-angle grain boundaries, identified

by ADF-STEM imaging, have been shown to considerably modify the Dirac states in Bi_2Se_3.[67]

WHAT IS NEXT?

While many excellent results have been reported on the crystalline structure and defects in tetradymite TIs using atomic-resolution STEM, most of them have only taken advantage of direct ADF imaging of the structures and, in some cases, complemented it with compositional mapping using EDX and EELS. However, there are additional capabilities in atomic-resolution analytical STEMs that can be utilized to better characterize and understand these tetradymite TIs. Notably, a wealth of information is present in the EELS data.[68] For example, by measuring the core-level electronic excitations, local variations in the electronic band structure of the material can be evaluated and understood.[69,70] These measurements could be particularly useful for the TI materials in which the band structure at the surfaces and interfaces is different from those in the bulk due to the nature of these materials.[28,39,71–76] Using core-loss EELS data, it should be possible to measure the effects of interfaces and defects on the local electronic properties of TI films and to evaluate the stability of topological properties. Another only lightly explored capability of analytical STEM is the use of EELS for measuring low-energy (0 eV–50 eV) excitations accruing in the TI films.[66,77,78] Measuring plasmonic oscillations at the surfaces and interfaces of TIs will provide a great deal of knowledge about the localization and features of charge modulations in the metallic portions of these materials.[79,80] It will also make it possible to measure the dielectric properties of the material across the entire film, which is essential for the determination of the electrical and optical characteristics of the material. Using monochromated EELS, the local phonon modes can be measured in these films to determine the thermal transport across QLs, planar defects, and interfaces.[81,82] In particular, by probing the relationship between the local structure and exotic physical properties, many avenues exist for intriguing STEM-based discoveries in TIs. Recent advances in STEM instrumentation, in particular the development of ultrahigh-energy-resolution monochromators and single-electron-counting detectors, should make it possible to perform these measurements with very high precision. So far, this field has only glimpsed the tip of the iceberg.

ACKNOWLEDGMENTS

This project was supported by SMART, one of the seven centers of nCORE, a Semiconductor Research Corporation program, sponsored by NIST.

DATA AVAILABILITY

Data sharing is not applicable to this article as no new data were created or analyzed in this perspective.

REFERENCES

[1] B. A. Bernevig, T. L. Hughes, and S.-C. Zhang, Science **314**, 1757 (2006).
[2] M. Z. Hasan and C. L. Kane, Rev. Mod. Phys. **82**, 3045 (2010).
[3] H. Zhang, C.-X. Liu, X.-L. Qi, X. Dai, Z. Fang, and S.-C. Zhang, Nat. Phys. **5**, 438 (2009).
[4] Y. L. Chen, J. G. Analytis, J.-H. Chu, Z. K. Liu, S.-K. Mo, X. L. Qi, H. J. Zhang, D. H. Lu, X. Dai, Z. Fang, S. C. Zhang, I. R. Fisher, Z. Hussain, and Z.-X. Shen, Science **325**, 178 (2009).
[5] J. J. Heremans, R. J. Cava, and N. Samarth, Nat. Rev. Mater. **2**, 17049 (2017).
[6] A. R. Mellnik, J. S. Lee, A. Richardella, J. L. Grab, P. J. Mintun, M. H. Fischer, A. Vaezi, A. Manchon, E.-A. Kim, N. Samarth, and D. C. Ralph, Nature **511**, 449 (2014).
[7] D. C. Mahendra, R. Grassi, J. Y. Chen, M. Jamali, D. Reifsnyder Hickey, D. Zhang, Z. Zhao, H. Li, P. Quarterman, Y. Lv, M. Li, A. Manchon, K. A. Mkhoyan, T. Low, and J. P. Wang, Nat. Mater. **17**, 800 (2018).
[8] J. S. Lee, A. Richardella, D. Reifsnyder Hickey, K. A. Mkhoyan, and N. Samarth, Phys. Rev. B **92**, 155312 (2015).
[9] H. Wang, J. Kally, J. S. Lee, T. Liu, H. Chang, D. Reifsnyder Hickey, K. A. Mkhoyan, M. Wu, A. Richardella, and N. Samarth, Phys. Rev. Lett. **117**, 076601 (2016).
[10] P. E. Batson, N. Dellby, and O. L. Krivanek, Nature **418**, 617 (2002).
[11] P. D. Nellist, M. F. Chisholm, N. Dellby, O. L. Krivanek, M. F. Murfitt, Z. S. Szilagyi, A. R. Lupini, A. Borisevich, W. H. Sides, Jr., and S. J. Pennycook, Science **305**, 1741 (2004).
[12] K. A. Mkhoyan, P. E. Batson, J. Cha, W. J. Schaff, and J. Silcox, Science **312**, 1354 (2006).
[13] E. J. Kirkland, R. F. Loane, and J. Silcox, Ultramicroscopy **23**, 77 (1987).
[14] S. J. Pennycook and L. A. Boatner, Nature **336**, 565 (1988).
[15] S. J. Pennycook, Ultramicroscopy **30**, 58 (1989).
[16] O. L. Krivanek, M. F. Chisholm, V. Nicolosi, T. J. Pennycook, G. J. Corbin, N. Dellby, M. F. Murfitt, C. S. Own, Z. S. Szilagyi, M. P. Oxley, S. T. Pantelides, and S. J. Pennycook, Nature **464**, 571 (2010).
[17] J. S. Jeong, M. L. Odlyzko, P. Xu, B. Jalan, and K. A. Mkhoyan, Phys. Rev. B **93**, 165140 (2016).
[18] M. Bosman, V. J. Keast, J. L. García-Muñoz, A. J. D'Alfonso, S. D. Findlay, and L. J. Allen, Phys. Rev. Lett. **99**, 086102 (2007).
[19] K. Kimoto, T. Asaka, T. Nagai, M. Saito, Y. Matsui, and K. Ishizuka, Nature **450**, 702 (2007).
[20] D. A. Muller, L. F. Kourkoutis, M. Murfitt, J. H. Song, H. Y. Hwang, J. Silcox, N. Dellby, and O. L. Krivanek, Science **319**, 1073 (2008).
[21] A. J. D'Alfonso, B. Freitag, D. Klenov, and L. J. Allen, Phys. Rev. B **81**, 100101 (2010).
[22] J. S. Jeong and K. A. Mkhoyan, Microsc. Microanal. **22**, 536 (2016).
[23] P. Kumar, *Structural Investigation of Electron-Beam Sensitive Zeolites and Metal–Organic-Frameworks Using Analytical Transmission Electron Microscopy* (University of Minnesota, 2018).
[24] J. S. Jeong, M. Topsakal, P. Xu, B. Jalan, R. M. Wentzcovitch, and K. A. Mkhoyan, Nano Lett. **16**, 6816 (2016).
[25] N. V. Tarakina, S. Schreyeck, T. Borzenko, C. Schumacher, G. Karczewski, K. Brunner, C. Gould, H. Buhmann, and L. W. Molenkamp, Cryst. Growth Des. **12**, 1913 (2012).
[26] N. V. Tarakina, S. Schreyeck, M. Luysberg, S. Grauer, C. Schumacher, G. Karczewski, K. Brunner, C. Gould, H. Buhmann, R. E. Dunin-Borkowski, and L. W. Molenkamp, Adv. Mater. Interfaces **1**, 1400134 (2014).
[27] Y. F. Lee, R. Kumar, F. Hunte, J. Narayan, and J. Schwartz, Acta Mater. **95**, 57 (2015).
[28] D. Reifsnyder Hickey, J. G. Azadani, A. R. Richardella, J. C. Kally, J. S. Lee, H. Chang, T. Liu, M. Wu, N. Samarth, T. Low, and K. A. Mkhoyan, Phys. Rev. Mater. **3**, 061201(R) (2019).
[29] D. L. Medlin, Q. M. Ramasse, C. D. Spataru, and N. Y. C. Yang, J. Appl. Phys. **108**, 043517 (2010).
[30] S. Borisova, J. Krumrain, M. Luysberg, G. Mussler, and D. Grützmacher, Cryst. Growth Des. **12**, 6098 (2012).
[31] H. S. Shin, S. G. Jeon, J. Yu, Y.-S. Kim, H. M. Park, and J. Y. Song, Nanoscale **6**, 6158 (2014).
[32] J. Kampmeier, S. Borisova, L. Plucinski, M. Luysberg, G. Mussler, and D. Grützmacher, Cryst. Growth Des. **15**, 390 (2015).

[33]Y. Liu, Y. Y. Li, D. Gilks, V. K. Lazarov, M. Weinert, and L. Li, Phys. Rev. Lett. **110**, 186804 (2013).
[34]P. Schönherr, D. Kojda, V. Srot, S. F. Fischer, P. A. Van Aken, and T. Hesjedal, APL Mater. **5**, 086110 (2017).
[35]M. Eschbach, M. Lanius, C. Niu, E. Młyńczak, P. Gospodarič, J. Kellner, P. Schüffelgen, M. Gehlmann, S. Döring, E. Neumann, M. Luysberg, G. Mussler, L. Plucinski, M. Morgenstern, D. Grützmacher, G. Bihlmayer, S. Blügel, and C. M. Schneider, Nat. Commun. **8**, 14976 (2017).
[36]K.-C. Kim, J. Lee, B. K. Kim, W. Y. Choi, H. J. Chang, S. O. Won, B. Kwon, S. K. Kim, D.-B. Hyun, H. J. Kim, H. C. Koo, J.-H. Choi, D.-I. Kim, J.-S. Kim, and S.-H. Baek, Nat. Commun. **7**, 12449 (2016).
[37]F. Lüpke, S. Just, G. Bihlmayer, M. Lanius, M. Luysberg, J. Doležal, E. Neumann, V. Cherepanov, I. Ošt'ádal, G. Mussler, D. Grützmacher, and B. Voigtländer, Phys. Rev. B **96**, 035301 (2017).
[38]J. H. Dycus, R. M. White, J. M. Pierce, R. Venkatasubramanian, and J. M. LeBeau, Appl. Phys. Lett. **102**, 081601 (2013).
[39]D. Reifsnyder Hickey, R. J. Wu, J. S. Lee, J. G. Azadani, R. Grassi, M. Dc, J. P. Wang, T. Low, N. Samarth, and K. A. Mkhoyan, Phys. Rev. Mater. **4**, 011201(R) (2020).
[40]A. Ghasemi, D. Kepaptsoglou, A. I. Figueroa, G. A. Naydenov, P. J. Hasnip, M. I. J. Probert, Q. Ramasse, G. Van der Laan, T. Hesjedal, and V. K. Lazarov, APL Mater. **4**, 126103 (2016).
[41]K. Sobczak, P. Strak, P. Kempisty, A. Wolos, A. Hruban, A. Materna, and J. Borysiuk, Phys. Rev. Mater. **2**, 044203 (2018).
[42]A. Ghasemi, D. Kepaptsoglou, L. J. Collins-McIntyre, Q. Ramasse, T. Hesjedal, and V. K. Lazarov, Sci. Rep. **6**, 26549 (2016).
[43]M. Jamali, J. S. Lee, J. S. Jeong, F. Mahfouzi, Y. Lv, Z. Zhao, B. Nikolic, K. A. Mkhoyan, N. Samarth, and J.-P. Wang, Nano Lett. **15**, 7126 (2015).
[44]Q. L. He, X. Kou, A. J. Grutter, G. Yin, L. Pan, X. Che, Y. Liu, T. Nie, B. Zhang, S. M. Disseler, B. J. Kirby, W. Ratcliff, Q. Shao, K. Murata, X. Zhu, G. Yu, Y. Fan, M. Montazeri, X. Han, J. A. Borchers, and K. L. Wang, Nat. Mater. **16**, 94 (2017).
[45]S. Borisova, J. Kampmeier, M. Luysberg, G. Mussler, and D. Grützmacher, Appl. Phys. Lett. **103**, 081902 (2013).
[46]F. Lüpke, M. Eschbach, T. Heider, M. Lanius, P. Schüffelgen, D. Rosenbach, N. Von Den Driesch, V. Cherepanov, G. Mussler, L. Plucinski, D. Grützmacher, C. M. Schneider, and B. Voigtländer, Nat. Commun. **8**, 15704 (2017).
[47]S. Schreyeck, N. V. Tarakina, G. Karczewski, C. Schumacher, T. Borzenko, C. Brüne, H. Buhmann, C. Gould, K. Brunner, and L. W. Molenkamp, Appl. Phys. Lett. **102**, 041914 (2013).
[48]A. Richardella, A. Kandala, J. S. Lee, and N. Samarth, APL Mater. **3**, 083303 (2015).
[49]L. He, X. Kou, M. Lang, E. S. Choi, Y. Jiang, T. Nie, W. Jiang, Y. Fan, Y. Wang, F. Xiu, and K. L. Wang, Sci. Rep. **3**, 3406 (2013).
[50]P. Tsipas, E. Xenogiannopoulou, S. Kassavetis, D. Tsoutsou, E. Golias, C. Bazioti, G. P. Dimitrakopulos, P. Komninou, H. Liang, M. Caymax, and A. Dimoulas, ACS Nano **8**, 6614 (2014).
[51]N. Koirala, M. Brahlek, M. Salehi, L. Wu, J. Dai, J. Waugh, T. Nummy, M.-G. Han, J. Moon, Y. Zhu, D. Dessau, W. Wu, N. P. Armitage, and S. Oh, Nano Lett. **15**, 8245 (2015).
[52]J.-Y. Hwang, Y.-M. Kim, K. H. Lee, H. Ohta, and S. W. Kim, Nano Lett. **17**, 6140 (2017).
[53]M. Lang, M. Montazeri, M. C. Onbasli, X. Kou, Y. Fan, P. Upadhyaya, K. Yao, F. Liu, Y. Jiang, W. Jiang, K. L. Wong, G. Yu, J. Tang, T. Nie, L. He, R. N. Schwartz, Y. Wang, C. A. Ross, and K. L. Wang, Nano Lett. **14**, 3459 (2014).
[54]Q. L. He, G. Yin, A. J. Grutter, L. Pan, X. Che, G. Yu, D. A. Gilbert, S. M. Disseler, Y. Liu, P. Shafer, B. Zhang, Y. Wu, B. J. Kirby, E. Arenholz, R. K. Lake, X. Han, and K. L. Wang, Nat. Commun. **9**, 2767 (2018).
[55]Y. T. Fanchiang, K. H. M. Chen, C. C. Tseng, C. C. Chen, C. K. Cheng, S. R. Yang, C. N. Wu, S. F. Lee, M. Hong, and J. Kwo, Nat. Commun. **9**, 223 (2018).
[56]Y. Zhao, M. de la Mata, R. L. J. Qiu, J. Zhang, X. Wen, C. Magen, X. P. A. Gao, J. Arbiol, and Q. Xiong, Nano Res. **7**, 1243 (2014).
[57]D. M. Kepaptsoglou, D. Gilks, L. Lari, Q. M. Ramasse, P. Galindo, M. Weinert, L. Li, G. Nicotra, and V. K. Lazarov, Microsc. Microanal. **21**, 1151 (2015).
[58]E. S. Kim, J. Y. Hwang, K. H. Lee, H. Ohta, Y. H. Lee, and S. W. Kim, Adv. Mater. **29**, 1604899 (2017).
[59]R. Yue, Y. Nie, L. A. Walsh, R. Addou, C. Liang, N. Lu, A. T. Barton, H. Zhu, Z. Che, D. Barrera, L. Cheng, P. R. Cha, Y. J. Chabal, J. W. P. Hsu, J. Kim, M. J. Kim, L. Colombo, R. M. Wallace, K. Cho, and C. L. Hinkle, 2D Mater. **4**, 045019 (2017).
[60]J. Liang, Y. J. Zhang, X. Yao, H. Li, Z.-X. Li, J. Wang, Y. Chen, and I. K. Sou, Proc. Natl. Acad. Sci. U. S. A. **117**, 221 (2020).
[61]M. Eschbach, E. Młyńczak, J. Kellner, J. Kampmeier, M. Lanius, E. Neumann, C. Weyrich, M. Gehlmann, P. Gospodarič, S. Döring, G. Mussler, N. Demarina, M. Luysberg, G. Bihlmayer, T. Schäpers, L. Plucinski, S. Blügel, M. Morgenstern, C. M. Schneider, and D. Grützmacher, Nat. Commun. **6**, 8816 (2015).
[62]M. Lanius, J. Kampmeier, C. Weyrich, S. Kölling, M. Schall, P. Schüffelgen, E. Neumann, M. Luysberg, G. Mussler, P. M. Koenraad, T. Schäpers, and D. Grützmacher, Cryst. Growth Des. **16**, 2057 (2016).
[63]A. Ghasemi, D. Kepaptsoglou, P. L. Galindo, Q. M. Ramasse, T. Hesjedal, and V. K. Lazarov, NPG Asia Mater. **9**, e402 (2017).
[64]N. V. Tarakina, S. Schreyeck, M. Duchamp, G. Karczewski, C. Gould, K. Brunner, R. E. Dunin-Borkowski, and L. W. Molenkamp, CrystEngComm **19**, 3633 (2017).
[65]K. Park, K. Ahn, J. Cha, S. Lee, S. I. Chae, S.-P. Cho, S. Ryee, J. Im, J. Lee, S.-D. Park, M. J. Han, I. Chung, and T. Hyeon, J. Am. Chem. Soc. **138**, 14458 (2016).
[66]S. C. Liou, M. W. Chu, R. Sankar, F. T. Huang, G. J. Shu, F. C. Chou, and C. H. Chen, Phys. Rev. B **87**, 085126 (2013).
[67]Y. Liu, Y. Y. Li, S. Rajput, D. Gilks, L. Lari, P. L. Galindo, M. Weinert, V. K. Lazarov, and L. Li, Nat. Phys. **10**, 294 (2014).
[68]R. Egerton, *Electron Energy-Loss Spectroscopy in the Electron Microscope*, 3rd ed. (Springer, New York, 2011).
[69]D. Muller, D. Singh, and J. Silcox, Phys. Rev. B **57**, 8181 (1998).
[70]L. J. Allen, S. D. Findlay, and M. P. Oxley, in *Scanning Transmission Electron Microscopy: Imaging and Analysis*, edited by S. J. Pennycook and P. D. Nellist (Springer, New York, NY, USA, 2011), pp. 247–289.
[71]S. K. Mishra, S. Satpathy, and O. Jepsen, J. Phys.: Condens. Matter **9**, 461 (1997).
[72]S. J. Youn and A. J. Freeman, Phys. Rev. B **63**, 085112 (2001).
[73]P. Larson, S. D. Mahanti, and M. G. Kanatzidis, Phys. Rev. B **61**, 8162 (2000).
[74]W. Liu, X. Peng, X. Wei, H. Yang, G. M. Stocks, and J. Zhong, Phys. Rev. B **87**, 205315 (2013).
[75]O. V. Yazyev, J. E. Moore, and S. G. Louie, Phys. Rev. Lett. **105**, 266806 (2010).
[76]P. Larson, V. A. Greanya, W. C. Tonjes, R. Liu, S. D. Mahanti, and C. G. Olson, Phys. Rev. B **65**, 085108 (2002).
[77]N. Talebi, C. Ozsoy-Keskinbora, H. M. Benia, K. Kern, C. T. Koch, and P. A. Van Aken, ACS Nano **10**, 6988 (2016).
[78]Y. Zhou, S. Liou, M. Lee, C. J. Klingshirn, X. Ge, W. C. H. Kuo, and G. Shu, Appl. Phys. Lett. **116**, 182108 (2020).
[79]H. Raether, *Surface Plasmons on Smooth and Rough Surfaces and on Gratings* (Springer, Berlin, 1988).
[80]J. Daniels, C. Festenberg, H. Raether, and K. Zeppenfeld, in *Springer Tracts in Modern Physics*, edited by G. Höhler (Springer, Berlin, 1970), Vol. 54, p. 77.
[81]M. J. Lagos, A. Trügler, U. Hohenester, and P. E. Batson, Nature **543**, 529 (2017).
[82]K. Venkatraman, B. D. A. Levin, K. March, P. Rez, and P. A. Crozier, Nat. Phys. **15**, 1237 (2019).